

General Disclaimer

One or more of the Following Statements may affect this Document

- This document has been reproduced from the best copy furnished by the organizational source. It is being released in the interest of making available as much information as possible.
- This document may contain data, which exceeds the sheet parameters. It was furnished in this condition by the organizational source and is the best copy available.
- This document may contain tone-on-tone or color graphs, charts and/or pictures, which have been reproduced in black and white.
- This document is paginated as submitted by the original source.
- Portions of this document are not fully legible due to the historical nature of some of the material. However, it is the best reproduction available from the original submission.

Aerospace Report No.
ATR-85(7083)-8

TWO-DIMENSIONAL QUASINEUTRAL DESCRIPTION
OF PARTICLES AND FIELDS ABOVE
DISCRETE AURORAL ARCS

Prepared by
A. L. Newman, Y. T. Chiu, and J. M. Cornwall
Space Sciences Laboratory

15 July 1985

Laboratory Operations
THE AEROSPACE CORPORATION
El Segundo, Calif. 90245

Prepared for
NATIONAL AERONAUTICS AND SPACE ADMINISTRATION
Headquarters, Washington, D.C.

Contract No. NASW-3839

(NASA-CR-176170) TWO-DIMENSIONAL
QUASINEUTRAL DESCRIPTION OF PARTICLES AND
FIELDS ABOVE DISCRETE AURORAL ARCS
(Aerospace Corp., El Segundo, Calif.) 44 p
HC 203/MF A01


N85-35517

Unclas
CSCL 04A 63/46 22248

Report No.
ATR-85(7083)-8

TWO-DIMENSIONAL QUASINEUTRAL DESCRIPTION
OF PARTICLES AND FIELDS ABOVE
DISCRETE AURORAL ARCS

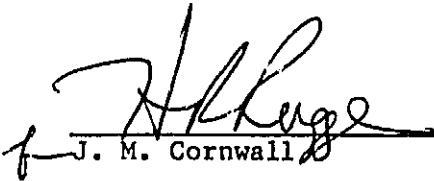
Prepared



A. L. Newman

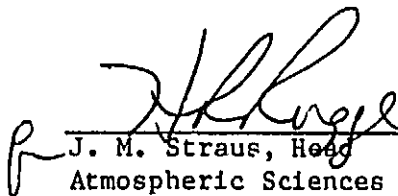


Y. T. Chiu

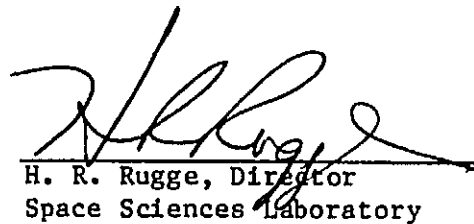


J. M. Cornwall

Approved



J. M. Straus, Head
Atmospheric Sciences Department



H. R. Ruge, Director
Space Sciences Laboratory

PRECEDING PAGE BLANK NOT FILMED

ABSTRACT

Stationary hot and cool particle distributions in the auroral magnetosphere are modelled using adiabatic assumptions of particle motion in the presence of broad-scale electrostatic potential structure. The study has identified geometrical restrictions on the type of broadscale potential structure which can be supported by a multispecies plasma having specified sources and energies. Without energization of cool thermal ionospheric electrons, a substantial parallel potential drop cannot be supported down to altitudes of 2000 km or less. Observed upward directed field-aligned currents must be closed by return currents along field lines which support little net potential drop. In such regions the plasma density appears significantly enhanced. Model details agree well with recent broad-scale implications of satellite observations.

PRECEDING PAGE BLANK NOT FILMED

CONTENTS

ABSTRACT.....	v
1. INTRODUCTION.....	1
2. TWO-DIMENSIONAL ELECTROSTATIC MODEL.....	7
3. SMOOTH SOLUTIONS—SPECIES DENSITIES AND ELECTROSTATIC POTENTIAL.....	19
4. IMPLICATIONS FOR PARTICLE HEATING.....	31
5. DISCUSSION.....	35
REFERENCES.....	37

PRECEDING PAGE BLANK NOT FILMED

FIGURES

1. A Schematic Diagram Summarizing Typical Observations and Interpretations Along Adjacent Evening Flux Tubes of Auroral Field Lines for Upward and Downward (Return) Current, Respectively.....	2
2. Regions of Velocity Space Occupied by Electrons of Magnetospheric Origin, Which Either Mirror Back Up Diverging Field Lines or Precipitate Toward the Lower Ionosphere.....	11
3. Boundaries in Velocity Space for Various Particle Populations at an Intermediate Position Along a Field Line in a Region of Upward Current.....	13
4. Boundaries in Velocity Space as per Figure 3, However, for a Reversed Parallel Potential Drop, Hence a Return Current Region.....	14
5. Computational Solutions for a) the Electrostatic Potential (kev) and b) Total Electron Density (/cc) Along a Geomagnetic Meridional Plane.....	20
6. Solutions for the Density (/cc) of electrons a) of Magnetospheric Origin, b) Trapped Along Flux Tubes, c) of Ionospheric Origin.....	22
7. Solutions for the Density (/cc) of Ions: a) Protons of Magnetospheric Origin, b) Protons of Ionospheric Origin, c) Oxygen Ions of Ionospheric Origin.....	26
8. Solutions for a) the Electrostatic Potential Versus Horizontal Distance, and b) the Potential Drop ($\phi_0 - \phi$) Versus Distance.....	29
9. Representations of O^+ and H^+ Distributions near Their Ionospheric Origin in a) an Upward Current Region, b) a Return Current Region with Reversed Potential Drop.....	32

PREVIOUS PAGE BLANK NOT VIEWED

TABLE

1. Parameters Defining the Particle Species for Six
Quasineutral Solutions..... 18

PREVIOUS PAGE BLANK NOT FILMED

1. INTRODUCTION

Over the past decade a quantitative description of the auroral quiet-time magnetosphere has been compiled from a large data base of satellite and ground-based observations (see Chiu et al., 1983; Burch et al., 1983; Mizera et al., 1981; Robinson et al., 1982; and many others). Large scale features are represented schematically in Fig. 1. Detailed analysis of data from such sources has resulted in significant progress toward the identification and interpretation of plasma boundaries, particle energy and flux characteristics, electrostatic wave generation, and indeed, the entire spectrum of magnetospheric phenomena.

The carriers of the large-scale Birkeland current linking the ionosphere and the magnetosphere have typically been identified as precipitating auroral electrons in the upward-current region and escaping thermal electrons in the downward-current regions (Anderson and Vondrak, 1975; Klumpar, 1979). Both species coexist, however, and often low-energy (< 50 eV) electrons can balance about half the primary upward current (Maier et al., 1980). Narrowly collimated electron beams are often seen at the edges of auroral arcs (Anderson, 1979), at energies below the parallel potential drop within inverted-V's (Burch et al., 1979, Lin and Hoffman, 1979); and in the cusp (Zanetti et al., 1981). Upward-flowing and counter-streaming (100 eV) electron beams have recently been described by Lin et al., (1982, 1984) and by Sharp et al. (1980). There is some evidence to suggest that imbalances in the counterstreaming fluxes provide the effective field-aligned current flow in these cases, and that the width in pitch angle of the upward electron flux increases with increasing electron energy. Burch et al. (1983) show that the pitch angle spread is related to the altitude of the top of a parallel potential drop below the spacecraft.

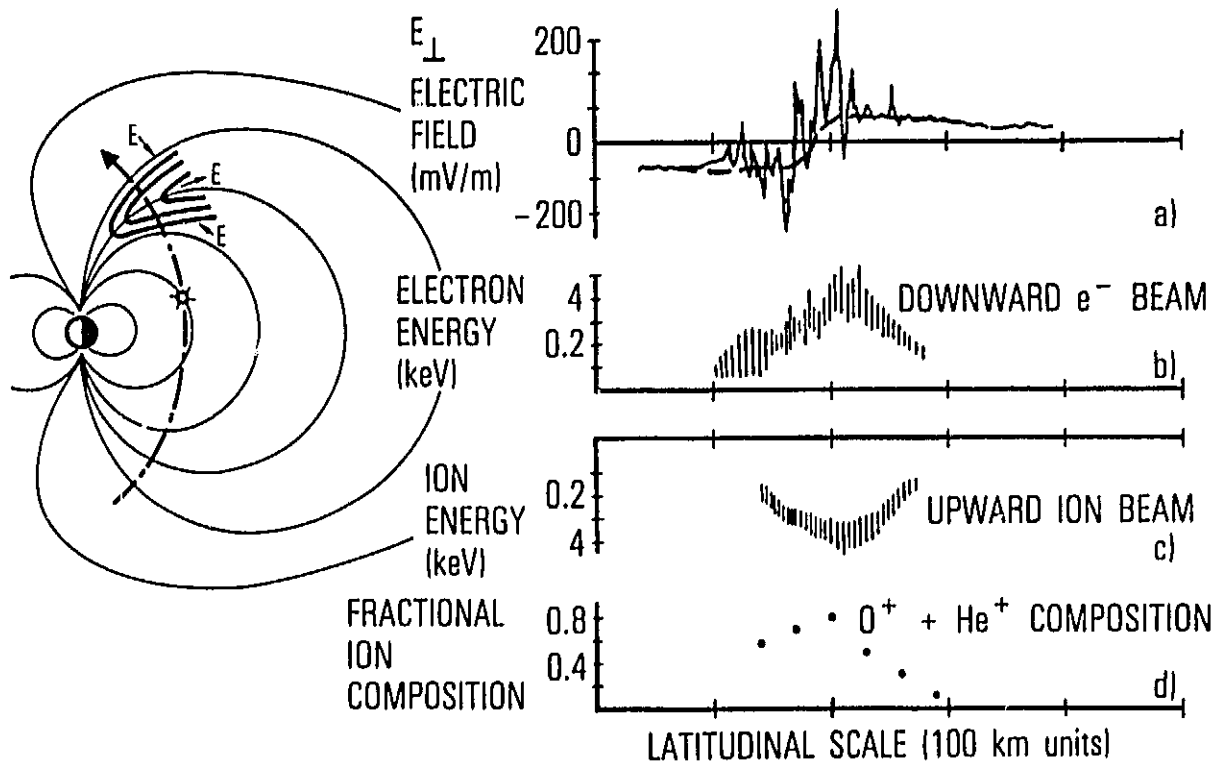


Figure 1. A Schematic Diagram Summarizing Typical Observations and Interpretations Along Adjacent Evening Flux Tubes of Auroral Field Lines for Upward and Downward (Return) Current, Respectively.

Johnston and Winningham (1982) and Klumpar and Heikkila (1982) also reported upward electron beams, the latter observations imbedded in a very broad region of downward Birkeland current. Collin et. al. (1982) showed that the occurrence frequency of upward beams is roughly eight times higher above 6000 km than below 3000 km; suggesting a sporadic (nonadiabatic) low-altitude acceleration mechanism while a steady mechanism (perhaps a broad-scale potential drop) dominates near 6000 km.

Similarly, observations of ions in upward-current regions have identified conic (transversely-accelerated) ion distributions with energies of greater than 500 eV at a few thousand km altitude (Sharp et. al. 1977), while upward ion beams are seen primarily above 6000 km (Gorney et. al., 1981). Lower energy conic ion distributions were observed to originate at lower altitudes irrespective of local time or parallel current direction (Gorney et. al., 1981; Whalen et. al., 1978; Klumpar, 1979; Horwitz et. al., 1981, 1982; Collin et. al. 1982). It is believed that the conic distributions are indicative of localized (1000 km thick) regions of non-adiabatic ion heating, while the upward ion beams reflect electrostatic acceleration by upward-directed parallel electric fields. Both mechanisms may act simultaneously (Klumpar et al., 1984).

Due to the highly variable nature of the medium, individual data sets are often analyzed in terms of the local environment only. Nevertheless, it has been well established (Lemaire and Scherer, 1973, 1983; Mizera et al., 1981; Chiu et al., 1983) that, for undisturbed conditions, the shapes of observed particle distributions are readily recovered by simple kinetic models which conserve the first two adiabatic invariants along auroral field lines. Kinetic theory qualitatively reproduces observed loss-cone, beam and conic features of individual particle species above 1000 km altitude.

In this paper, observed features of particle distribution functions along auroral magnetospheric field lines are reproduced by a two-dimensional stationary model. The model is initialized by a representation of cross-field potential structure suggested by Chiu et al. (1981) as a solution allowing current closure within a finite domain of closed field lines. Simple bi-Maxwellian distribution functions (as in the one-dimensional study of Chiu and Schulz, 1978) have been adiabatically mapped along field lines, taking into account acceleration due to monotonic parallel potential drops. The distribution functions are then integrated in velocity space to provide particle densities as functions of magnetic induction and electrostatic potential for eight species of ionized particles. Shooting techniques are employed to identify smooth solutions for the electrostatic potential which satisfy quasi-neutrality everywhere.

Section 2 describes the model and techniques for providing satisfactory solutions for the auroral potential structure. Density variations for eight particle populations are limited by adiabatic invariant boundaries in velocity space, and by effective particle temperatures, while they appear to be largely insensitive to our choice of bi-Maxwellian distributions. While such a simple direct model cannot accurately represent details of particle heating processes and pitch angle diffusion, these effects are induced through increased particle temperatures and the existence of trapped particles. Hence, recognizing that significant electric fields are responsible for localized nonadiabatic heating, we employ model representations of ionospheric species which are assumed to behave adiabatically after experiencing heating in a low altitude acceleration region.

Section 3 focuses on new interpretations based on these solutions. Our two-dimensional model results predict density cavities along field lines which

support large potential drops (as seen by Calvert, 1981), and conversely, density enhancements along field lines which have no potential drop (i.e., at the edges of inverted V's as seen by Anderson, 1979). In regions of upward current, quasineutrality demands that any parallel potential drop along the lowest few thousand kilometers of the field line must be of the same order of magnitude as the temperature of the cool electron species. We show, in fact, that both the breadth and shape of the low altitude electrostatic potential structure appear to depend strongly on the energy of a population of cool electrons of ionospheric origin. In general, we expect that the potential drop along the lower part of a field line is never much greater than the temperature of the ionospheric species retarded by that potential.

The concluding section provides interpretations of the distinct features of the model in terms of satellite observations, and discusses implications of the model in regions of sharp density gradients at the edges of observed inverted-V events. The model will be shown to represent well the salient features of the data, including prominent features predicted by the model and only recently experimentally confirmed. These features include the identification of cool electrons of ionospheric origin as the current carriers in the low altitude return current region, enhancement in the density of most species along field lines which do not support a significant potential drop, and a strong correlation between the effective temperatures of particle species originating in the ionosphere and the depth of penetration of V-shaped potential structures into the ionosphere.

2. TWO-DIMENSIONAL ELECTROSTATIC MODEL

As in earlier studies [e.g., Chiu and Schulz (1978)], the particle motion is constrained in the magnetosphere by the conservation of energy and magnetic moment along field lines:

$$W \equiv \frac{m}{2} (v_{\parallel}^2 + v_{\perp}^2) + q|e| \phi \quad (1)$$

$$\mu \equiv m v_{\perp}^2 / (2B), \quad (2)$$

where W is the total energy, m is the particle mass, $q (= +$ or $- 1)$ is the particle charge in units of the electron charge $|e|$. v_{\parallel} , v_{\perp} are particle velocities parallel and perpendicular to the magnetic field, respectively ($v_{\parallel} > 0$ is downward). ϕ and B are the electrostatic potential and magnetic field magnitude, respectively.

The simplest particle distribution functions are characterized at a convenient point of origin as bi-Maxwellians:

$$f \propto \exp (W_{\parallel} / T_{\parallel} + W_{\perp} / T_{\perp})$$

or

$$f \propto \exp \left[\frac{m}{2} \left(\frac{v_{\parallel}^2}{T_{\parallel}} + \frac{v_{\perp}^2}{T_{\perp}} \right) + q|e| \frac{\phi}{T_{\parallel}} \right]. \quad (3)$$

Once the effective temperatures and electrostatic potential are determined at one point, which we designate as the "source" of the particle distribution, then the adiabatic invariants associated with the conservation of energy and

magnetic moment completely determine the particle distribution at every other point along the magnetic field line -- as long as the electrostatic potential is known everywhere.

Boundary conditions are of great importance. Assuming conjugate-point symmetry along field lines, we define the upper boundary of the system to be the magnetospheric equator, the source region for hot plasma sheet protons and electrons. Particles traveling downward which reach the lower boundary are presumed to be lost from the system. The lower boundary at the base of the field lines is assumed to be an ionospheric sink (or source) located high enough that particle collisions may be neglected. We have chosen 1000 km altitude as the altitude in our model at which ambipolar diffusion is no longer dominant and magnetospheric quasineutrality limits particle flux.

The region below 1000 km is complex due to collisional effects. To avoid complicating our representation of the magnetospheric plasma, we chose this altitude as a lower boundary characterized by an ionospheric source which models the low altitude plasma. Cool ions below 1000 km altitude, which are gravitationally and collisionally bound, slow the escape of electrons up the field lines. An effective upward-directed electric field component is generated by ambipolar diffusion in this region. Note that this region effectively restricts most of the ionospheric particles to the ionosphere because only the most energetic can escape. This also answers a complaint voiced by early opponents to the idea of higher altitude parallel electric fields directed downward; scientists who felt that such fields would evacuate the ionosphere. The ionosphere is preserved because downward electric fields do not extend through the ionosphere to the earth's surface. (The reversed potential drops will be examined in detail in work to be presented elsewhere.) Gradual heating of the ion and electron populations occurs as

electrons are energized by the precipitating flux, and ions are energized by perpendicular field turbulence in the form of wave/particle interactions.

In this paper we sidestep the question of low-altitude local heating mechanisms to address the question of the accumulated affect of this heating on the high altitude distributions. How hot must the ionospheric species be in order to provide a quasineutral plasma at high altitude with the distribution function boundaries seen by satellites in these regions? Our cooler ionospheric distributions in this report represent only those particles which could escape the ionosphere, that is, superthermal particles.

The bi-Maxwellian distribution functions are further restricted by an imposed accessibility criterion which states that the parallel velocity as defined by (1) must be real at the source, and at all positions along a field line between the source and any position, s , where the density is nonzero. This states that a particle cannot pass through a region where the probability of particle occurrence is zero. Note that even abrupt monotonic changes in the electric field are acceptable as long as the particle is accessible to the point of interest.

Particle velocity-space distribution functions are restricted to specific regions of velocity-space by imposed boundary conditions and adiabatic invariants. The adiabatic invariants relate the velocity distribution at a boundary to that at any position s (see Chiu and Schulz, 1978; recall that ions require an extra term to include the effect of gravity):

$$v_{\parallel \ell}^2 = v_{\parallel s}^2 + [1 - (B_{\ell}/B_s)] v_{\perp s}^2 + (2q|e|/m_e) (\phi_s - \phi_{\ell}) \quad (5)$$

Hence, the boundary limitations ($s = \ell, 0$) may be plotted in velocity space for any particle at position s , where ℓ refers to the lower boundary and 0 to the magnetospheric equator. This is illustrated in Fig. 2 for hot magnetospheric electrons accelerated by a 2 keV drop in the potential along the length of a field line. The hot electrons are restricted to the region outside the ellipse $v_{\parallel 0}^2 = 0$; that is, all must have access to their point of origin at $s = 0$. The hyperbola, $v_{\parallel \ell}^2 = 0$, separates sections of velocity space occupied by particles of magnetospheric origin which mirror, from that occupied by particles which precipitate. In applying these boundary conditions, particles which mirror before they reach the lower boundary ($v_{\parallel \ell}^2 < 0$) are distinguished from those which precipitate through the lower boundary and are lost ($v_{\parallel s} > 0, v_{\parallel \ell}^2 > 0$).

As shown in Fig. 2a, most hot electrons (of several keV) near the origin are mirroring electrons (cross-hatched area). When a parallel potential drop of 2 keV is assumed along the field line, much more of velocity space is accessible near the top of the field line (Fig. 2a) than at lower altitudes (Fig. 2b). A large fraction of those electrons which are able to approach the bottom boundary (Fig. 2c) also have a high downward ($v_{\parallel} > 0$) parallel component of velocity and will precipitate. Electrons which pass down the field lines through a sizeable potential drop (upward E_{\parallel}) are all accelerated to higher speeds, leaving the central ellipse of the distribution function empty (see Fig. 2c); describing partial ring distributions. The ellipse is not filled by electrons streaming out of the ionosphere because upward motion of cooler electrons is effectively curtailed by the potential drop. The realization of this fact led researchers to interpret observed inverted-V events as distinct signatures of parallel potential drops. If, however, mechanisms exist to energize these cool electrons to 50-2000 eV, electron conics are seen travelling obliquely up the field lines [Menietti and Burch, 1985].

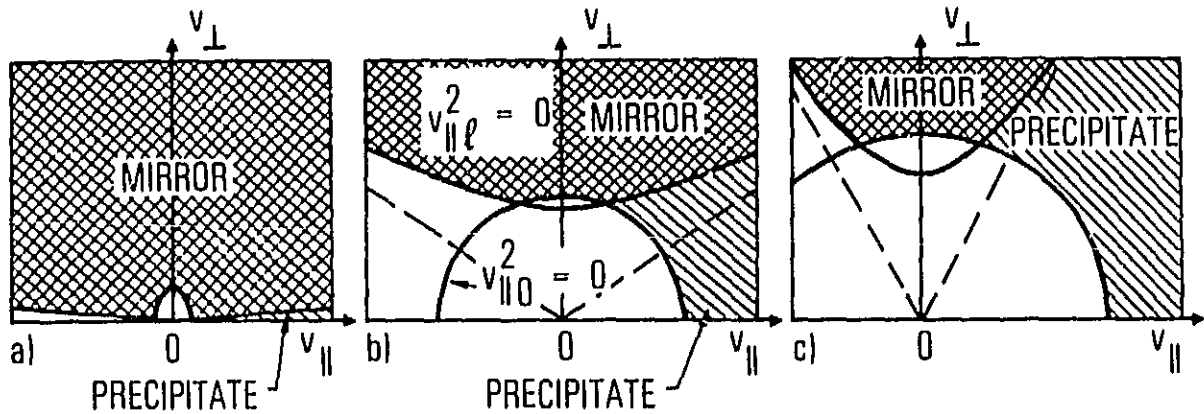


Figure 2. Regions of Velocity Space Occupied by Electrons of Magnetospheric Origin, Which Either Mirror Back Up Diverging Field Lines or Precipitate Toward the Lower Ionosphere. A potential drop of 2 keV is assumed along the field line. Regions are shown for particle distributions a) near the source of particles (magnetospheric equator); b) at an intermediate position; and c) near the base of the field line (assumed to be at altitude of about 1000 km).

In observed particle velocity-space distributions non-adiabatic processes (e.g., pitch-angle diffusion) smooth the edges of the boundaries in velocity space. Nevertheless, it is possible to distinguish contributions to different regions, bounded by these curves as shown in Fig. 3a for ions, and Fig. 3b for electrons. If downward-directed electric fields exist, the boundary curves for ions and electrons are reversed as shown in Fig. 4. Typical distributions sample mixed populations of both hot and cool particles; the hot particles originating near the plasma sheet while the cooler particles have their source in the ionosphere. Assuming that the particles conserve adiabatic invariants, estimates of the potential drop necessary to produce observed distribution functions are routinely made from satellite data (Mizera et. al., 1981; Chiu et. al., 1982).

Here we extend the theory to describe particle distributions along the entire length of magnetic field lines across the auroral zone. The densities of all representative particle populations are obtained by integrating over adiabatically allowed regions of velocity space and applying shooting techniques to solve for values of the electrostatic potential which satisfy quasineutrality among the particle densities at every point in space. These models contain both regions of upward current and regions of return current in order to preserve charge balance between the magnetosphere and ionosphere.

Our technique for achieving self-consistent solutions requires initial estimates of the two-dimensional potential structure. The structure along the top boundary (magnetospheric equator) is assumed to be a smoothly-varying function of cross-field distance. By choosing a simple potential well, we have been able to confirm analytically our numerical solutions for the potential at the lower boundary which satisfy current continuity within the system (Chiu et. al., 1981). Conceivably, any potential structure could be

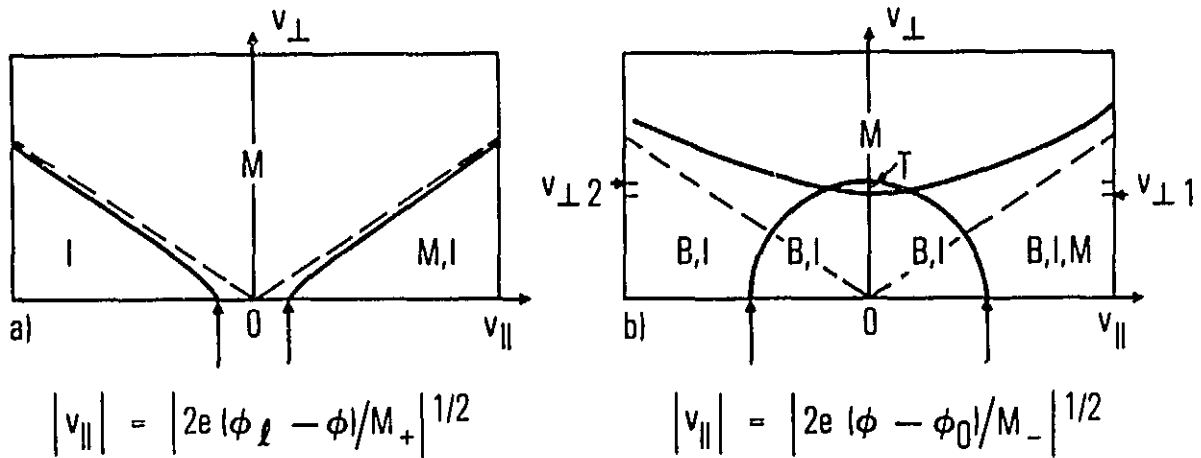


Figure 3. Boundaries in Velocity Space for Various Particle Populations at an Intermediate Position Along a Field Line in a Region of Upward Current. The species are either a) ions, or b) electrons designated by M if they are assumed to originate in the plasmasheet (magnetosphere), and by I if the assumed origin is the ionosphere. B designates backscattered electrons, and T designates electrons trapped between converging magnetic field lines and a parallel potential barrier. The dashed diagonal lines are asymptotes $v_{\parallel} = \pm_2 [B_{\ell}/B - 1]^{1/2} v_{\perp}$ of the solid hyperbolic boundary $v_{\parallel \ell} = 0$.

$$v_{\perp 1} \equiv \left[\frac{2}{m_{-}} \left(\frac{e(\phi_{\ell} - \phi)}{B_{\ell}/B - 1} \right) \right]^{1/2}, \quad v_{\perp 2} \equiv \left[\frac{2}{m_{-}} \left(\frac{e(\phi - \phi_0)}{1 - B_0/B} \right) \right]^{1/2}$$

[From Chiu and Schulz, 1978]. The scale size for ion velocities is ten times the electron velocity scale.

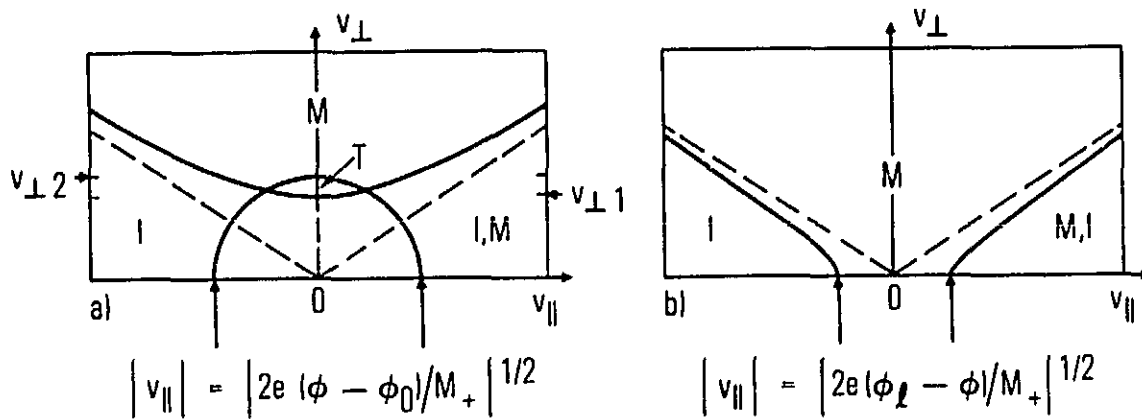


Figure 4. Boundaries in Velocity Space as per Figure 3, However, for a Reversed Parallel Potential Drop, Hence a Return Current Region. The region designated T indicates that trapped ions may exist at some positions along a field line. The scale size for ion velocities is one hundred times the electron velocity scale of Figure 3. $v_{\perp 1}$ and $v_{\perp 2}$ have the form given in Figure 3 with m_- replaced by m_+ .

applied at the upper boundary; our simple choice is based on an understanding of typical length scales across auroral field lines near the equator. For the ionospheric potential ϕ_p , the height-integrated current continuity equations reduce to

$$\nabla_{\perp} \cdot (\Sigma_p \nabla_{\perp} \phi_p) = -J_{\parallel}$$

where J_{\parallel} is defined as negative for downgoing electrons and Σ_p is the height-integrated Pederson conductivity. Kinetic models and observations imply that J_{\parallel} is proportional to the field-aligned potential difference between the magnetospheric equator and the ionosphere. By estimating the proportionality constant, one can express the current conservation equation as a Poisson-like equation which allows us to estimate the potential structure at the lower boundary (as in Chiu et al., 1981). An interpolation linear in B then provides an initial estimate of the electrostatic potential everywhere between the boundaries. This interpolation procedure is chosen because the kinetic-theory proportionality of potential to J_{\parallel} along a field line, yields a potential proportional to B , which leads to a current conserved without transverse components. Recent experimental observations by both DE spacecraft along the same field line confirm this proportionality [Weimar, 1985].

Once the potential is estimated everywhere, the particle density functions are obtained by integrating the distribution functions over allowed regions of velocity space for all representative particle populations. These density functions depend only on magnetic field, electrostatic potential, effective particle temperatures (parallel and perpendicular to the magnetic field), and on a constant multiplicative coefficient defined by boundary conditions. At the upper boundary a balance is assumed between the densities

of oppositely-charged particles of plasma sheet origin. At the lower boundary, a similar condition forces charge neutrality among particles of ionospheric origin. Initial estimates of the densities are made for a variety of particle temperatures within the energy ranges suggested by satellite data. The total charge density is calculated on a coarse grid between the boundaries, and parameter sets describing the particle temperatures and density coefficients are chosen for which quasineutral solutions appear likely at all spatial positions.

Quasineutral solutions are quite adequate for the range of parameters of interest in the evening magnetosphere, as long as variations on spatial scales comparable to the ion Larmor radius are not of concern [Chiu et al. (1983)]. Sharp variations in the electric field are not of interest because they would invalidate the assumptions of adiabaticity inherent in our model. The smoothly-varying large-scale potential structure described by our model is representative of the net charge separation and E_{\parallel} associated with inverted-V structures, where the actual net charge density on auroral field lines is very small. If a quasineutral solution could not be obtained everywhere across such a large-scale system, then it would also be unlikely that the derived particle densities could adequately describe a steady, quiet magnetosphere. Reasonable solutions are in fact identified, particle densities are calculated at each point on a fine grid, and shooting techniques are used to refine the value of the potential until quasineutrality is achieved at each grid point to within an absolute error, $2|n_+ - n_-|/(n_+ + n_-)$, of 0.001 or less.

A few statements must be included here to address the uniqueness of the solutions and the ease in obtaining them. We have found that once species' temperatures and coefficients are defined and boundary conditions are applied, then there will be either one physically meaningful solution, or none. Our

system of constraints is too rigid to allow an unreasonable solution. It is feasible, for example, that shooting techniques could converge on a value of the potential inappropriate for low altitudes, in an attempt to balance, say, cool ions with trapped electrons rather than with cool electrons when the latter are too cold to be accessible to these heights. Invariably, in such cases the technique fails miserably near the lower boundary, and further efforts must be extended to find appropriate cool electron temperatures. A single solution at any point is not necessarily unique; however, a smooth consistent solution everywhere may often be obtained by predisposing the shooting technique to search for a solution near the value computed at the same altitude for an adjacent field line. Any discontinuous solutions are rejected as inconsistent with adiabatic invariant assumptions. The parameters listed in Table 1 are representative of typical solutions which satisfy quasineutrality everywhere. The evening magnetosphere may adopt one of a number of steady configurations, differing in representative temperatures of different species, and in the shape of net potential structure.

Table 1. Parameters Defining the Particle Species for Six Quasineutral Solutions

Particle Species/ Parameter	Example					
	1	2	3	4	5	6
n_{I-}						
T_{\parallel}	1.2	40	1	2	.4	.8
T_{\perp}	1.2	40	2	2	.4	.8
$C(x10^{-34})$	76	13	41	59	45	45
n_{H+}						
T_{\parallel}	0.5	0.6	0.7	5	.03	.03
T_{\perp}	10	20	20	5	.03	.03
$C(x10^{-35})$	3.9	2.1	2.3	25	3.4×10^8	3.4×10^8
n_{O+}						
T_{\parallel}	1	3	5	10	.15	.35
T_{\perp}	15	20	50	10	.15	.35
$C(xC_{H+})$	30	71	34	23	4.2	4.2
n_{B-}						
T	16	400	400	400	300	300
C	0.34	0.34	0.34	0.34	0.34	0.34
n_{T-}						
T	1500	1000	1000	1500	400	400
C	61	40	32	83	64	64
Upward Current Solution	X	X	X	X		
Return Current Solution					X	X

Temperatures are in eV. Multiplicative coefficients = C_S in cc^{-1} depend on distribution function form. n_{M+} is isotropic with $T=6$ keV. n_{M-} is anisotropic in the upward current region with $T_{\parallel} = 1.5$ keV and $T_{\perp} = 3$ keV at the central field line; but isotropic in the return current region with $T=2.5$ keV, (see text). $C_{M+} = 1.1 \times 10^{-33}$; $C_{M-} = 2.8 \times 10^{-38}$.

3. SMOOTH SOLUTIONS - SPECIES DENSITIES AND ELECTROSTATIC POTENTIAL

We will consider in detail several sets of quasineutral solutions. The particle parameters differ for regions of upward or return current but are otherwise constant. Table 1 lists parameters describing quasineutral multicomponent plasma species under various magnetospheric conditions. The effective temperatures quoted describe a bi-Maxwellian distribution for each species only at its source. Further along the field line adiabatic invariants may impose a highly asymmetric distribution. Two sets of parameters are used to define a standard magnetosphere, the choice of upward and return current parameters determined by the requirement that the total upward current balance the total downward current of the complete system. (The current density is $2.6 \mu\text{A}/\text{m}^2$ at the base of the field line carrying the strongest upward current.)

In Fig. 5, examples 1 and 5 from Table 1 for the two current regions are compared with examples 2 and 6. Both electrostatic potential and total plasma density are computed on a representative 12×46 point grid in a meridional plane across the auroral zone. The model calculations employ dipolar geometry, however, for clearer illustration we have plotted the results employing the familiar transformation $x = x_0 (B_0/2B_\rho)^{1/2}$, compressing divergent field lines to parallel vertical lines with the magnetospheric equator at the top boundary and 1000 km ionospheric altitude at the bottom. The cross-field distance scale refers to distances between field lines at the lower boundary (the baropause at 1000 km altitude). The transformation acts as an image enhancement, readily identifying gradients in the potential or density with respect to the magnetic field geometry. The shaded central portion of each plot identifies a region of upward current surrounded by unshaded symmetric return current regions. Note that the physics does not specify whether return

ORIGINAL PAGE IS
OF POOR QUALITY

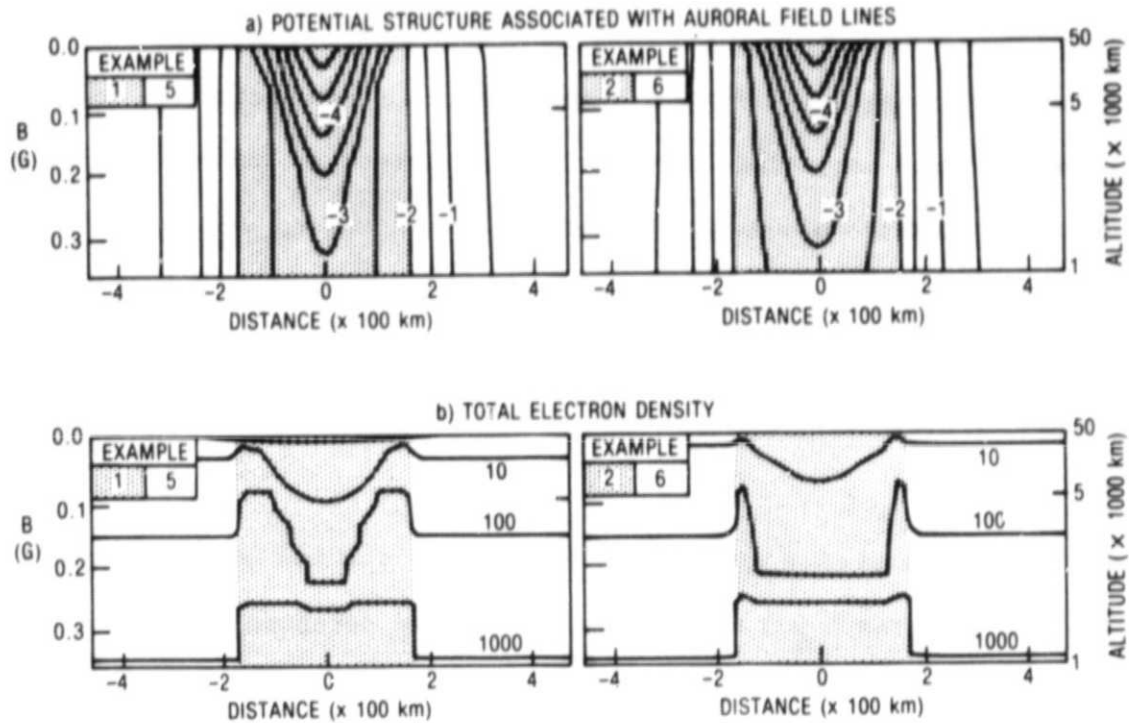


Figure 5. Computational Solutions for a) the Electrostatic Potential (kev) and b) Total Electron Density (/cc) Along a Geomagnetic Meridional Plane. Magnetic field lines are plotted as vertical lines in this projection. As labelled, the upward current regions (shaded) are described by Table 1 examples 1 and 2. Similarly, the unshaded regions are symmetric return current regions described in Table 1 by examples 5 and 6.

currents should be north or south of an upward current region. Certainly both are seen, so we include both in our representations.

Fig. 5 illustrates the kind of broad-scale variations to be expected in satellite observations. Narrow potential structures which become increasingly narrow at lower altitudes may be seen in conjunction with localized plasma density cavities which become smaller at lower altitudes. Broader and deeper potential structure correlates with more extensive plasma depletions, bounded by very narrow density enhancements. The character of specific solutions stems directly from the response of individual particle species to the global electric and magnetic field structure.

Fig. 6 illustrates the density variation of three separate electron populations. The hot electrons of magnetospheric origin are isotropic (2.5 keV) in the return current region, but are allowed to become gradually anisotropic toward the central field line where $(T_{\parallel}, T_{\perp}) = (1.5, 3)$ keV. This feature has been incorporated to match interpretations of observed velocity-space anisotropies, but it has only a minor effect on the density structure of the hot electrons, and practically no effect on quasineutrality considerations. These hot electrons are most dense at their origin, the top boundary of Fig. 6a. The electrons are least dense in the central region where they are accelerated downward by a potential drop of 2600 eV, and many are lost due to precipitation through the lower boundary. Reduced precipitation along equipotential field lines near the outer edges of the upward current region produce a density maximum there. The return current region is assumed to support a small parallel potential drop which is assumed by us to be steady over hundreds of kilometers, producing a constant density versus latitudinal distance. The return current potential drop is characteristic of an extended ambipolar potential, and is sufficient to

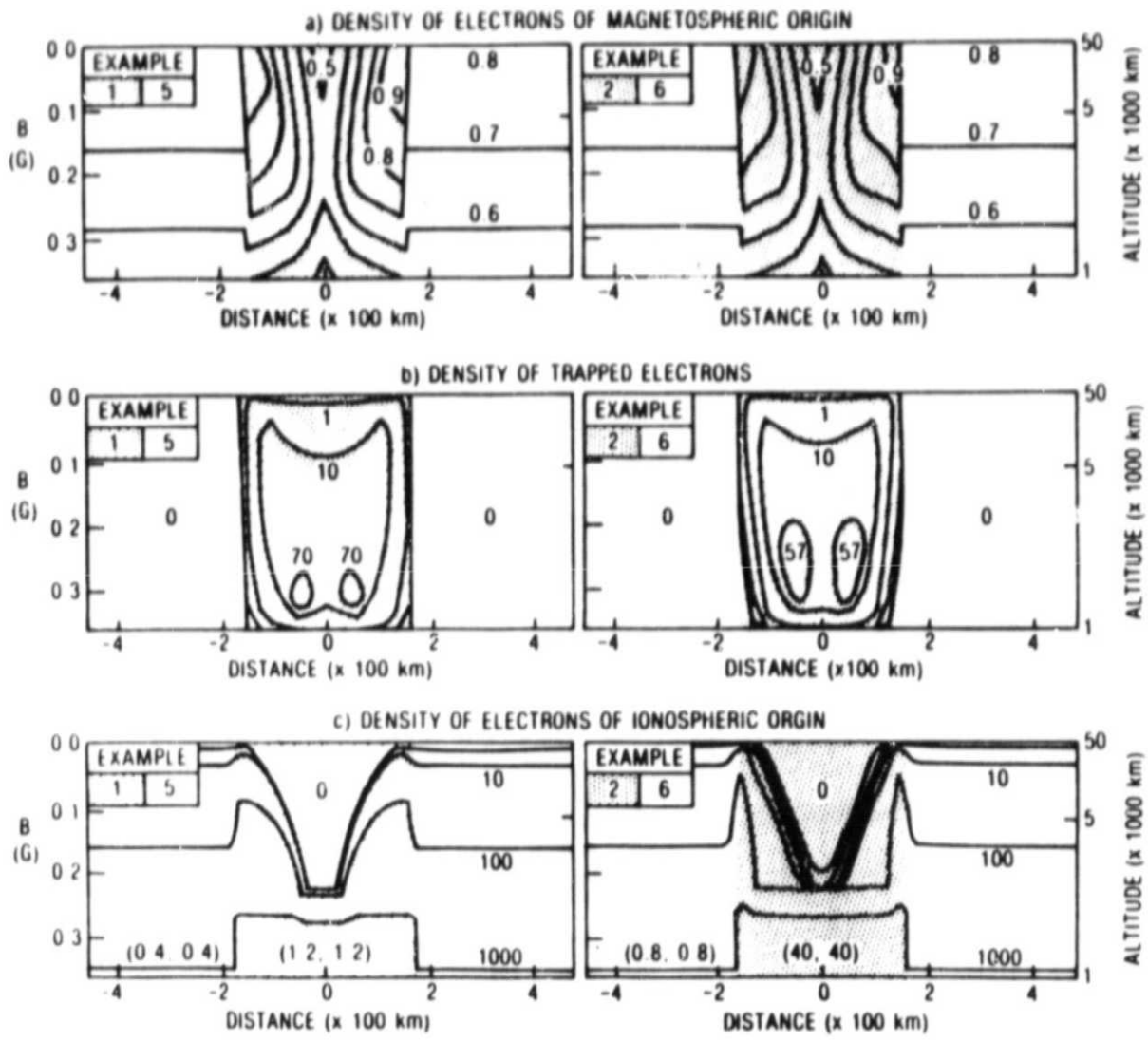


Figure 6. Solutions for the Density (/cc) of electrons a) of Magnetospheric Origin, b) Trapped Along Flux Tubes, c) of Ionospheric Origin. Numbers in brackets denote Maxwellian temperatures (T_{\parallel} , T_{\perp}) at the species origin in the upward or return current regions as indicated. The format is as given in Figure 5.

balance the upward current when the sum of the small currents carried by each field line is evaluated.

Trapped electrons (Fig. 6b) occupying the region of velocity space labelled T in Fig. 3, are restricted to the upward current region and are most dense near the lower boundary. Double maxima occur on either side of the central field line at several thousand kilometers altitude. The central minimum between the maxima in the density contours of Fig. 6b occurs because the central field lines carry a more significant potential drop to very low altitudes, hence further restricting the allowed region of velocity space for trapped particles along these field lines. Technically, there is no mechanism to produce trapped particles in a completely adiabatic system, but we know that diffusive processes tend to fill restricted areas of velocity space. We assume that the population exists, and that it is maintained by the gradual diffusion of electrons across boundaries in velocity space; a minor perturbation on an otherwise stationary adiabatic system. The model solutions for the trapped electron distribution functions suggest that these are basically electrons of ionospheric origin which have received significant transverse acceleration at low altitude and have diffused upward into a region where they are trapped adiabatically between a potential barrier at high altitude and the dipolar magnetic mirror at low altitude.

Untrapped electrons of ionospheric origin are represented in Fig. 6c. These electrons are so dense at low altitudes that they essentially determine the net character of density gradients in the plasma as a whole. The numbers in brackets above the lower boundary are the effective bi-Maxwellian parallel and perpendicular temperatures (isotropic for these examples) defining this cool electron population at the lower boundary. In both examples given, the assumed temperatures are superthermal. The order-of-magnitude difference in

their temperatures accounts for the difference in the gradients of both plasma density and potential of Fig. 5. The maximum in this electron distribution is always at the outer edge of the upward current region along field lines which support no potential drop.

In the upward current region where cool ions are accelerated upward by the central parallel potential drop, it is necessary to have a mechanism to allow a sufficient number of cool electrons to follow the ions so that quasineutrality is satisfied between these dense, cool ionospheric populations at low altitudes. Very cool electrons cannot cross a significant potential barrier, so the low altitude potential drop must be very small in the first example of Fig. 6c. Warmer electrons can penetrate further into a significant potential structure; or, to look at the phenomena another way, the potential structure can penetrate lower in the magnetosphere without retarding the ionospheric electrons too severely. In both examples, a density minimum in this population occurs along the field lines supporting the largest potential drop. Such density cavities have been observed by Calvert (1981) and others. They suggest that density cavities are correlated with observations of auroral kilometric radiation (AKR), possibly identifying source regions for electron cyclotron energization. In the examples of Fig. 5 the central density cavities do meet the threshold condition for AKR; that is, the plasma frequency is less than one fifth of the electron cyclotron frequency. Warm electron distributions within the density depletion appear conic-like as observed recently by Menietti and Burch (1985). If the potential drop is small, dipolar magnetic field geometry causes cooler electron distributions to appear to be upward-travelling beams or counter-streaming beams above 3000 - 4000 km, agreeing with observations of Lin et al. (1984) and Sharp et al. (1980).

One might expect an important role to be played by another electron population energized at low altitudes through backscattering by hot precipitating electrons. Backscattered electrons are included in the model, based on predictions of Prasad et al. (1983). These predictions suggest a maximum density of less than 0.5 particles per cc, that is, too small to significantly affect quasineutrality. The backscattered electron density contours are not plotted in Fig. 6 because they are a very minor component. The density contours have similar shape to scaled trapped electron predictions without the central minimum. Cool ionospheric, trapped, and backscattered electrons all serve to neutralize the accelerated ionospheric ions streaming upward in the region of upward current. Distinguishing between these electron populations is difficult experimentally. The ionospheric electrons and backscattered electrons occupy the same region of phase space and are hence indistinguishable from each other on the scales of importance here. Our models indicate only that warmer-than-thermal electrons are necessary to achieve a quasineutral state in the 1000 - 4000 km region. Our representation of the balance between backscattered and cooler electrons may be considered tentative, in lieu of more quantitative data which is able to distinguish between them. It is clear, however, that if the potential drop extends to great depth in the ionosphere some nonadiabatic process must exist which transfers sufficient energy to the cool electrons to allow them to reach adequate heights following the accelerated ions.

The most important ion populations corresponding to the electrons of Fig. 6 are illustrated in Fig. 7. The magnetospheric ions in the model are assumed to be isotropic at temperatures of 6 keV. These ions are only slightly retarded by the potential drop, the lowest density seen in the center of the upward current region. Trapped ions may also exist but only in the return

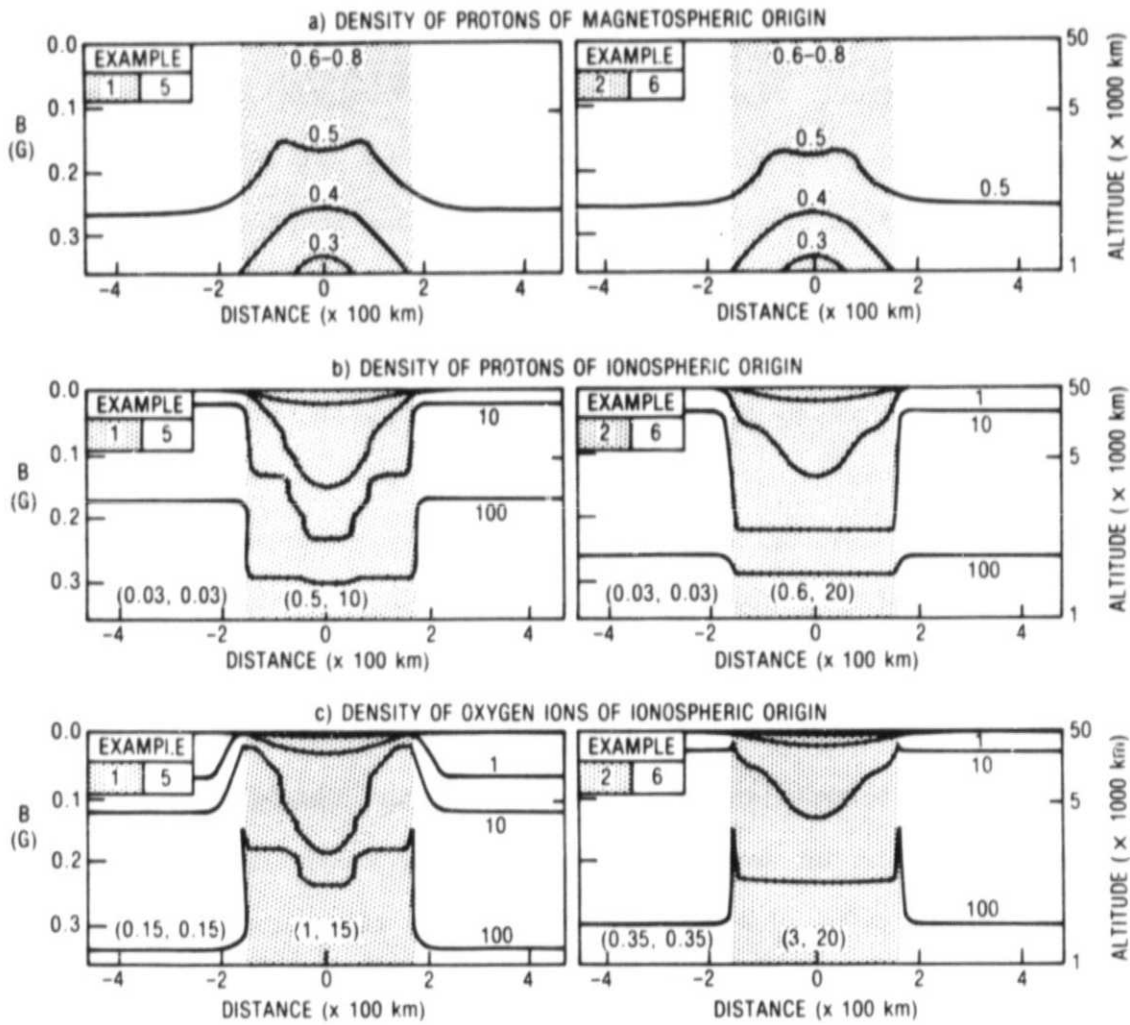


Figure 7. Solutions for the Density (/cc) of Ions: a) Protons of Magnetospheric Origin, b) Protons of Ionospheric Origin, c) Oxygen Ions of Ionospheric Origin. The format is as given in Fig. 6.

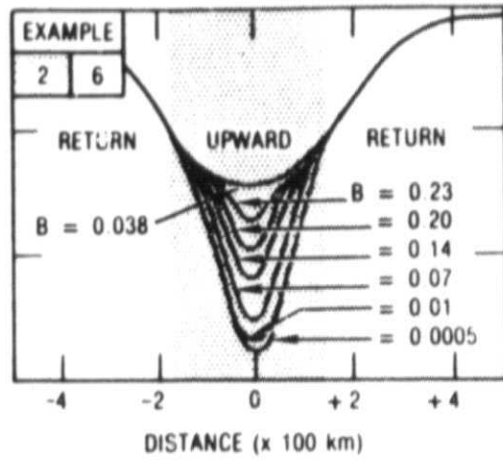
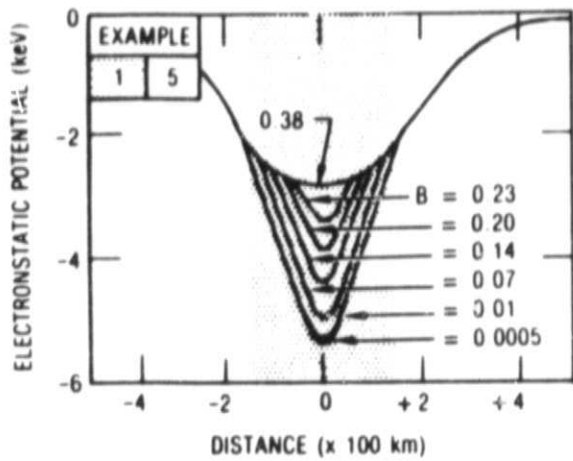
current regions which support a reversed parallel potential drop. Even within a reverse potential drop it is unlikely that they have a major role in charge balance. Observations of low energy ions indicate beam and conic shaped distributions rather than the shape predicted for trapped distributions in Fig. 4a. Although some argument can be made that the observed ions are the result of non-adiabatic heating events at magnetospheric altitudes of 1000-5000 km altitude, it is clear that the bulk of the distributions seen do not correlate with trapped ion distributions along field lines above a localized heating region. The beam and conic ions appear to map essentially adiabatically as warmed distributions of ions that are not significantly retarded by any potential barrier! One suggestion that comes to mind is that the sluggish ions absorb energy from local wave fields (through resonant, non-adiabatic processes which tend to deplete the wave field). The warmed ions are subsequently channelled by the dipolar magnetic field geometry into conic distributions at low altitudes and beam distributions at higher altitudes. Note that movements of localized field structure could cause variations in the height of the heating region for ions, and indeed many such regions could feasibly exist.

The resulting ion distributions can be modelled by recognizing that these effects tend to smooth the particle distributions. With minor distortions at very low altitude, the observed distributions are represented as somewhat warm populations of ions originating at low altitude. Both low-energy hydrogen and oxygen ions are assumed to exist. In the example of Fig. 7, highly anisotropic distributions were assumed in the central acceleration region with perpendicular temperatures exceeding parallel temperatures by factors of 7 to 33 as shown. These ions appear as beams and conics, originating near the lower boundary (1000 km altitude), after presumably having undergone

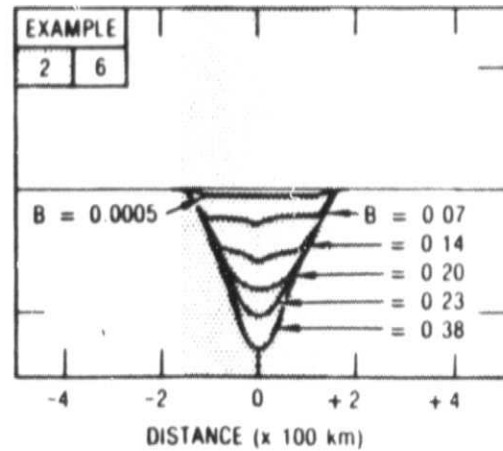
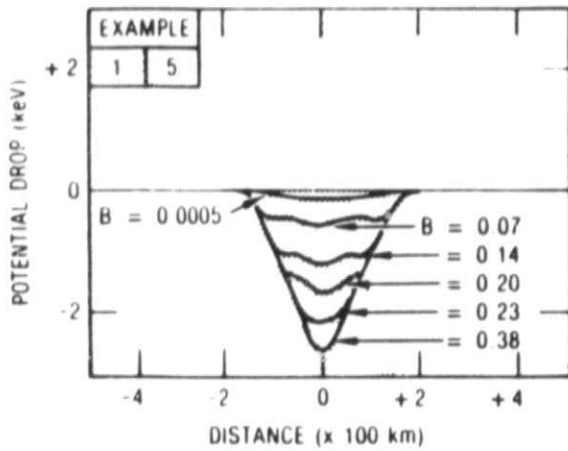
non-adiabatic heating in some altitude range near this boundary. Recall, the non-adiabatic process is not represented here, just the result of the process, that is, the existence of warmed ions.

The most distinct features of the ionospheric ion distributions shown in Fig. 7 are the sharp increases in the density along field lines which have no potential drop. Since these ions are not accelerated out of the region by an external electric field, they are more dense. Technically, there are more ions along these field lines because fewer are lost at the boundaries (more of velocity-space is assessible to them). In this model we consider the ionospheric source region at the bottom boundary to be a constant; hence, particles returning to the source do not supplement the source. The model thus predicts a steady-state distribution of ions with more ions attached to some field lines than others. (This same argument is seen to be valid also for the ionospheric electrons.) Other features of the model include a decrease in ion density along field lines supporting the largest potential drop. Both ions and electrons spend proportionately less time in such regions of strong electrostatic acceleration. Above about 2000 km the cool ionospheric electron population is excluded by strong fields in the central region, and the ionospheric ions and trapped electrons form a quasineutral balance.

The altitude above which cool ionospheric electrons are negligible differs in the two examples shown because of details in the low altitude potential structure. In Fig. 8a latitudinal variations in the electrostatic potential are plotted at constant values of the magnetic field (ie. essentially constant altitude). The base of the field line has a magnetic field of 0.38 G, while the magnetospheric equator is at 0.00053 G. Following a curve for a constant magnetic field of say 0.14 G (4000 km altitude) in.



a)



b)

Figure 8. Solutions for a) the Electrostatic Potential Versus Horizontal Distance, and b) the Potential Drop ($\phi_0 - \phi$) Versus Distance.

example 1/5, we see that the potential matches the lower boundary potential for all but the central half of the upward current region. That is, up to 4000 km the outer half of the field lines in the upward current region are equipotentials -- motion up the field lines is not impeded for any cool species, and particle densities are higher than they would otherwise be. In example 2/6, there is a small fairly constant potential drop in the same region. The more energetic part of the 40 eV cool ionospheric electron population could cross this small potential barrier. Quasineutrality is satisfied if there are not too many cool ions reaching this altitude. Fig. 6, 7 and 8 show that both electron and ion densities are lower in this region for example 2/6 than for example 1/5. Small variations in the potential drop at low altitude have a strong effect on the distribution of cooler particles at higher altitudes.

High altitude variations in the potential drop are more difficult to interpret. Fig. 8b illustrates variations in the potential drop from the top boundary as the auroral zone is crossed in the north-south direction. If a satellite maintained a constant altitude (approximately constant magnetic field) over several degrees latitude N-S distance, it would observe a fairly constant potential drop from the top boundary, throughout the central portion of the upward current region down to an altitude of about 4000 km ($B = 0.14G$). This does not suggest that downgoing particles of magnetospheric origin would contribute constant densities at a specific altitude in the central region. The structure near the top boundary in the graph of magnetospheric electrons (recall Fig. 6) is caused by mirroring hot electrons which are also influenced by the variable potential drop below this altitude. Nonetheless, one general rule which holds for all untrapped particle species is that lower density is found along field lines which support a significant potential drop.

4. IMPLICATIONS FOR PARTICLE HEATING

Observations of warm ion populations (conics) directed obliquely upward (Gorney et. al., 1981; and Klumpar, 1982) have helped to define the anisotropic ion distributions in our model. Recent observations have highlighted striking differences in the motion of different ion species [Hultqvist, 1983; Horwitz, 1982]. Differences in heating regions and heating rates are important; however, we can readily show that a factor at least as important is the difference in adiabatic motion of different species within static fields. This is well illustrated by plotting the boundary restrictions for both oxygen (dotted line) and hydrogen (solid curve) in regions for which an upward/downward (Fig. 9a/b) parallel electric field component exists between the field line position (s) and the ionospheric boundary. In an upward current region, as in Fig. 9a, individual hydrogen ions (H) would be accelerated to greater velocities by the potential drop than would the oxygen ions (O). In addition, oxygen ions must overcome a gravitational barrier sixteen times as great as for hydrogen ions, so the net accelerating potential is greater for the hydrogen ions. As a result, the hydrogen ions spend less time in the vicinity of position s , and would be less dense there (all other parameters being equal). Although the ratio of the densities of oxygen to hydrogen ions at the lower boundary is taken to be a half, the ratio increases to a maximum of 1.1 higher up the central field line over the arc. If ion heating occurred at low altitude, it is clear that the oxygen ions would spend much more time in this region than the hydrogen ions simply due to their slower parallel velocities. Local heating would thus allow an even greater proportion of oxygen to escape further along the field lines. Note that in the examples we consider, the accelerating potential drop extends down to the lower boundary over the central field line. If conditions were very quiet,

the potential drop would not extend as deep, and it is likely that a much less significant oxygen ion component would penetrate into the magnetosphere. Prognostic observations described by Hultqvist (1983) indicate that the oxygen to hydrogen ratio at geosynchronous altitudes may be a factor of ten or so during disturbed times. Horwitz (1982) also observes a stronger oxygen component at 1400 km for very disturbed cases only. Most often the potential drop does not extend deeper than 5000 km (Gorney et al., 1981) and the ratio is less than one. It is of interest that even in disturbed conditions the energy in the observed oxygen and hydrogen distributions (at geosynchronous altitudes) is about the same for both species; indicating that the dominant source of free energy is probably electrostatic in nature.

5. DISCUSSION

In this paper, we have described models of electrostatic potential distributions consistent with current continuity and charge balance, for particle populations governed by adiabatic invariants and quasineutrality in the magnetosphere. The models reproduce the general characteristics of quiet-time satellite observations over evening auroral arcs, both in regions of upward and return current. Estimates of the current density show that the upward current density above 1000 km is carried by a population of hot electrons of magnetospheric origin. (Although the trapped electrons may carry appreciable current in either direction, the net effect is zero.) Throughout the return current region, the current is carried by the cooler electrons of ionospheric origin. We also infer from the models that both the latitudinal extent of the electrostatic potential structure, as well as the depth of penetration of this accelerating potential into the ionosphere are strongly influenced by the effective energy of the cool electron population. Our modelling results conclude that broad potential structure extending low along the field lines can only describe a stationary quasineutral solution if the representative ionospheric electron population is assumed to be suprathermal (10 - 100 eV). Hence, signature of strong parallel electric field components seen to extend down to lower altitudes, could be interpreted as a sign that non-adiabatic heating of the cooler electrons had taken place. Thick regions of enhanced density at the outer edges of inverted-V's may indicate a cooler ionospheric electron distribution. In this case quasineutrality demands that the field-aligned potential drop be suppressed at low altitudes (allowing some cool electrons up the field lines to balance ions of ionospheric origin). This also tends to reduce the cross-field extent of the potential structure, allowing the magnetic field lines to appear as approximate equipotentials up to great altitudes.

REFERENCES

- Atkinson, G., Field-aligned current as a diagnostic tool: result a renovated model of the magnetosphere, *J. Geophys. Res.*, 89, 217-226, 1984.
- Benson, R. F. and W. Calvert, ISIS-1 observations at the source of auroral kilometric radiation, *Geophys. Res. Lett.*, 6, 479-482, 1979.
- Burch, J.L., P.H. Reiff, and M. Sugiura, Upward electron beams measured by DE-1: A primary source of dayside region-1 Birkeland currents, *Geophys. Res. Lett.*, 10, 753-756, 1983.
- Butler, D.M., ed. Connection between the magnetosphere and ionosphere, in *Solar Terrestrial Physics - Present and Future*, NASA - SPKXX, Ch. 7, U.S. Government Printing Office, Washington, D.C., in press, 1984.
- Calvert, W., The auroral plasma cavity, *Geophys. Res. Lett.*, 8, 919-921, 1981.
- Chiu, Y.T. and J.M. Cornwall, Electrostatic model of a quiet auroral arc, *J. Geophys. Res.*, 85, 543-556, 1980.
- Chiu, Y.T. and M. Schulz, Self-consistent particle and parallel electrostatic field distributions in the magnetospheric-ionospheric auroral region, *J. Geophys. Res.*, 83, 629-642, 1978.
- Chiu, Y.T., A.L. Newman, and J.M. Cornwall, On the structures and mapping of auroral electrostatic potentials, *J. Geophys. Res.*, 86, 10029-10036, 1981.
- Chiu, Y.T., J.M. Cornwall, J.F. Fennell, D.J. Gorney, and P.F. Mizera, Auroral plasmas in the evening sector: Satellite observations and theoretical interpretations, *Space Sci. Rev.* 35, 211-257, 1983.
- Collin, H.L., R.D. Sharp, and E.G. Shelley, The occurrence and characteristics of electron beams over the polar regions, *J. Geophys. Res.*, 87, 7504-7511, 1982.

- Fridman, M., and J. Lemaire, Relationship between auroral fluxes and field-aligned electric potential difference, *J. Geophys. Res.*, 85, 664-670, 1980.
- Goertz, C.K., and R.W. Boswell, Magnetosphere-ionosphere coupling, *J. Geophys. Res.*, 84, 7239-7246, 1979.
- Gorney, D.J., A. Clarke, D.R. Croley, Jr., J.F. Fennell, J.G. Luhmann, P.F. Mizera, Distribution of ion beams and conics above 8000 km., *J. Geophys. Res.*, 86, 0083-0089, 1981.
- Gorney, D.J., Y.-T. Chiu and D.R. Croley, Trapping of ion conics by parallel electric fields, *J. Geophys. Res.*, in press, 1984.
- Heelis, R.A., J.D. Winningham, M. Sigiura, and N.C. Maynard, Particle acceleration parallel and perpendicular to the magnetic field observed by DE-2, *J. Geophys. Res.*, 89, 3893-3902, 1984.
- Kan, J.R., Energization of auroral electrons by electrostatic shock waves, *J. Geophys. Res.*, 80, 2089-2095, 1975.
- Kan, J.R., and L.C. Lee, Theory of imperfect magnetosphere-ionosphere coupling, *Geophys. Res. Lett.*, 7, 633-636, 1980.
- Klumpar, D.M., and W.J. Heikkila, Electrons in the ionospheric source cone: evidence for runaway electrons as carriers of downward Birkeland currents, *Geophys. Res. Lett.*, 9, 873-876, 1982.
- Klumpar, D.M., W.K. Peterson and E.G. Shelley, Direct evidence for two-stage (bimodal) acceleration of ionospheric ions, *J. Geophys. Res.*, 89, 10779-10787, 1984.
- Lin, C.S., J.L. Burch, J.D. Winningham, J.D. Menietti, and R.A. Hoffman, DE-1 observations of counterstreaming electrons at high altitudes, *Geophys. Res. Lett.*, 9, 925-928, 1982.

- Lyons, L.R., Generation of large-scale regions of auroral currents, electric potentials, and precipitation by the divergence of the convection electric field, J. Geophys. Res., 85, 17-24, 1980.
- Lyons, L.R., and D.S. Evans, An association between discrete aurora and energetic particle boundaries, J. Geophys. Res., 89, 2395-2400, 1984.
- Lysak, R.L. and C. Dum, Dynamics of magnetosphere-ionosphere coupling including turbulent transport, J. Geophys. Res., 88, 365-380, 1983.
- Menietti, J.D., and J.L. Burch, "Electron Conic" signatures observed in the nightside auroral zone and over the polar cap, in publication, J. Geophys. Res., 1985
- Mitchell, H.G.Jr., and P.J. Palmadesso, A dynamic model for the auroral field line plasma in the presence of field-aligned current, J. Geophys. Res., 88, 2131-2139, 1983.
- Miura, A. and T. Sato, Numerical simulation of global formation of auroral arcs, J. Geophys. Res., 85, 73-91, 1980.
- Mizera, P.F., J.F. Fennell, D.R. Croley, Jr., and D.J. Gorney, Charged particle distributions and electric field measurements from S3-3, J. Geophys. Res., 86, 7566-7576, 1981.
- Oya, H., Results of satellites Kyokko (EXOS-A) and Jikiken (EXOS-B) dedicated to the study of auroral physics, Symposium on Achievements of the International Magnetospheric Study, XXV Cospar, Graz, Austria, 25 June -7 July, 1984.
- Prasad, S.S., D.J. Strickland, and Y.T. Chiu, Auroral electron interaction with the atmosphere in the presence of conjugate field-aligned electrostatic potentials, J. Geophys. Res., 88, 4123-4130, 1983.
- Rich, F.J., and Y. Kamide, Convection electric fields and ionospheric currents derived from model field-aligned currents at high latitudes, J. Geophys. Res., 88, 271-281, 1983.

- Robinson, R.M., R.R. Vondrak and T.A. Potemra, Electrodynamic properties of the evening sector ionosphere within the Region 2 field-aligned current sheet, 87, 731-741, 1982.
- Sato, T., A theory of quiet auroral arcs, J. Geophys. Res., 83, 1042-1048, 1978.
- Serizawa, Y. and T. Sato, Generation of large scale potential difference by currentless plasma jets along the mirror field, Geophys. Res. Lett., 11, 595-598, 1984.
- Sharp, R.D., E.G. Shelley, R.G. Johnson, and A.G. Ghielmetti, Counterstreaming electron beams at altitudes of $\approx 1 R_E$ over the auroral zone, J. Geophys. Res., 85, 92-100, 1980.
- Singh, N. and R.W. Schunk, Comparison of the characteristics of potential drop and current-driven double layers, J. Geophys. Res., 88, 10081-10090, 1983.
- Stern, D.W., One-dimensional models of quasi-neutral parallel electric fields, J. Geophys. Res., 86, 5839-5860, 1981.
- Swift, D.W., On the formation of auroral arcs and acceleration of auroral electrons, J. Geophys. Res., 80, 2096-2108, 1975.
- Torbert, R.B., and F.S. Mozer, Electrostatic shocks as the source of discrete auroral arcs, Geophys. Res. Lett., 5, 135-138, 1978.
- Weimar, D. R., C. K. Goertz, D. A. Gurnett, N. C. Maynard, and J. L. Burch, Auroral zone electric fields from DE-1 and DE-2 at magnetic conjunctions, submitted, 1985.